

1    **Host abundance and heterogeneity in infectiousness determine extent of the environmental  
2    reservoir**

3    Nichole A. Laggan<sup>1\*</sup>, Katy L. Parise<sup>2</sup>, J. Paul White<sup>3</sup>, Heather M. Kaarakka<sup>3</sup>, Jennifer A. Redell<sup>3</sup>,  
4    John E. DePue<sup>4</sup>, William H. Scullon<sup>5</sup>, Joseph Kath<sup>6</sup>, Jeffrey T. Foster<sup>2</sup>, A. Marm Kilpatrick<sup>7</sup>,  
5    Kate E. Langwig<sup>1</sup>, Joseph R. Hoyt<sup>1</sup>

6    <sup>1</sup>Department of Biological Sciences, Virginia Polytechnic Institute, Blacksburg, VA, 24060 USA

7    <sup>2</sup>Pathogen and Microbiome Institute, Northern Arizona University, Flagstaff, AZ, 86011, USA

8    <sup>3</sup>Wisconsin Department of Natural Resources, Madison, WI, 53707, USA

9    <sup>4</sup>Michigan Department of Natural Resources, Baraga, MI 49870, USA

10    <sup>5</sup>Michigan Department of Natural Resources, Norway, MI 49908, USA

11    <sup>6</sup>Illinois Department of Natural Resources, Springfield, IL, 62702, USA

12    <sup>7</sup>Department of Ecology and Evolutionary Biology, University of California, Santa Cruz, CA,  
13    95064, USA

14    **\*Correspondence to:** Nichole A. Laggan: [nicholelaggan@gmail.com](mailto:nicholelaggan@gmail.com)

15    **Key words:** emerging infectious disease, environmental pathogen reservoir, pathogen shedding,  
16    host infectiousness, environmental transmission, white-nose syndrome

17    **Open Research statement:** Data will be made available through the Dryad Digital Repository  
18    before publication or upon reviewer request.

19     **Abstract**

20           Environmental pathogen reservoirs exist for many globally important diseases and can  
21        fuel disease outbreaks, affect pathogen evolution, and increase the threat of host extinction.  
22        Differences in pathogen shedding among hosts can create mosaics of infection risk across  
23        landscapes by increasing pathogen contamination in high use areas. However, how the  
24        environmental reservoir establishes in multi-host communities and the importance of factors like  
25        host-specific infection and abundance in environmental contamination and transmission remain  
26        important outstanding questions. Here we examine how *Pseudogymnoascus destructans*, the  
27        fungal pathogen that causes white-nose syndrome in bats, invades and establishes in the  
28        environment. We quantified dynamic changes in pathogen shedding, infection intensities, host  
29        abundance, and the subsequent propagule pressure imposed by each species within the  
30        community. We find that the initial establishment of the pathogen reservoir is driven by different  
31        species within the community than those that are responsible for maintaining the reservoir over  
32        time. Our results also show that highly shedding species do not always contribute the most to  
33        pathogen reservoirs. More broadly, we demonstrate how individual host shedding rates scale to  
34        influence landscape-level pathogen contamination.

35 **Introduction**

36 Emerging infectious diseases threaten efforts to conserve global biodiversity (Daszak et  
37 al. 2000, Taylor et al. 2001, Jones et al. 2008, Fisher et al. 2012). In some disease systems,  
38 pathogens may survive for long periods of time in the environment in the absence of a living host  
39 (Turner et al. 2016, Plummer et al. 2018, Islam et al. 2020). Pathogen persistence in the  
40 environment allows for transmission independent of infected hosts, can exacerbate disease  
41 impacts, and increase the risk of host extinction (de Castro and Bolker 2005, Mitchell et al. 2008,  
42 Almberg et al. 2011, Hoyt et al. 2020). However, pathogen contamination in the environment is  
43 not homogenous, rather, variation in the extent of the environmental reservoir is likely driven by  
44 a complex process of pathogen shedding from hosts within the community that lead to  
45 subsequent transmission events.

46 Infected hosts can vary in the amount of pathogen they shed into the environment with  
47 some hosts producing disproportionately high amounts of pathogen, independent of host contacts  
48 (Sheth et al. 2006, Chase-Topping et al. 2008, Lawley et al. 2008, Direnzo et al. 2014). Research  
49 has shown that inherent variation in host shedding can be driven by differences in behavior  
50 (Godfrey 2013, Rushmore et al. 2013, VanderWaal and Ezenwa 2016), innate susceptibility  
51 (Searle et al. 2011, Gervasi et al. 2013), space use (Brooks-Pollock et al. 2014), and infection  
52 severity (Lloyd-Smith et al. 2005, Munywoki et al. 2015). In multi-host disease systems, the  
53 variation produced through community composition and species abundance play key roles that  
54 determine transmission dynamics (Kilpatrick et al. 2006, Paull et al. 2012).

55 Host abundance within a community can interact with host shedding to moderate  
56 transmission from a particular species (Lloyd-Smith et al. 2005, Paull et al. 2012, Kilonzo et al.  
57 2013). Species that have low rates of shedding, but are highly abundant, may contribute more to

58 transmission than might be expected based on the amount of pathogen they shed (Peterson and  
59 McKenzie 2014, Scheele et al. 2017). Conversely, a species that has high rates of shedding or is  
60 highly infectious, but at low abundance, may contribute less to transmission than other species  
61 (Lloyd-Smith et al. 2005, Kilpatrick et al. 2006). In addition, for some wildlife infectious  
62 diseases, infectiousness, shedding, and impacts are positively correlated (Langwig et al. 2016,  
63 Brannelly et al. 2020) such that hosts that are initially important in transmission suffer from high  
64 impacts and become less important contributors to the environmental reservoir over time.  
65 Heterogeneity in pathogen shedding and how it influences disease dynamics is important for  
66 many disease systems (Sheth et al. 2006, Chase-Topping et al. 2008, Henaux and Samuel 2011,  
67 Brooks-Pollock et al. 2014, Direnzo et al. 2014, Slater et al. 2016), but how differences in host  
68 shedding scale to a community-level and influence the environmental reservoir is rarely linked  
69 together.

70 White-nose syndrome (WNS) is an emerging infectious disease caused by the fungal  
71 pathogen *Pseudogymnoascus destructans* (Lorch et al. 2011, Warnecke et al. 2012), that has had  
72 devastating effects on bat populations (Langwig et al. 2012, Frick et al. 2015, Langwig et al.  
73 2016). White-nose syndrome exhibits seasonal infection dynamics that are driven by the  
74 environmental reservoir and host-pathogen ecology (Langwig et al. 2015a, Hoyt et al. 2021,  
75 Langwig et al. 2021). *Pseudogymnoascus destructans* can persist for long periods of time in the  
76 environment, which results in widespread infection when hosts return to hibernacula  
77 (subterranean sites where bats hibernate in the winter) in the fall (Lorch et al. 2013, Hoyt et al.  
78 2015, Langwig et al. 2015a, Campbell et al. 2019, Hoyt et al. 2020, Hicks et al. 2021). During  
79 this time, susceptible bats become infected or reinfected by *P. destructans* when they come into  
80 contact with the environmental reservoir upon entering hibernacula (Langwig et al. 2015a). Over

81 the winter hibernation period, *P. destructans* grows into the skin tissue, causing deleterious  
82 physiological changes, including increased arousals from hibernation, weight loss, dehydration,  
83 and ultimately death (Warnecke et al. 2013, Verant et al. 2014, McGuire et al. 2017, Hoyt et al.  
84 2021). During hibernation, susceptible bat species vary greatly in their infection intensities and  
85 three species have suffered declines that exceed 95% (Langwig et al. 2012, Langwig et al. 2016,  
86 Hoyt et al. 2020, Hoyt et al. 2021). While species vary in infection intensities, species abundance  
87 also varies greatly within bat communities (Langwig et al. 2012, Frick et al. 2015), which may  
88 also influence pathogen contamination in the environment.

89 Contamination of *P. destructans* in the environment increases after the first year of  
90 invasion (Hoyt et al. 2020) and the extent of the environmental reservoir has been linked to  
91 increased pathogen prevalence and increased pathogen loads for bats across the globe (Hoyt et  
92 al. 2020, Hoyt et al. 2021). As a result, bat mortality also increases with higher levels of  
93 environmental contamination (Hoyt et al. 2018, Hoyt et al. 2020, Hicks et al. 2021). However,  
94 how the environmental pathogen reservoir becomes established in these multi-host communities  
95 has not been investigated.

96 Environmental transmission is an important driver of infectious disease dynamics and  
97 understanding the factors that lead to pathogen establishment in the environment is crucial for  
98 disease control and prevention. Here we use a unique dataset that encompasses the stages of *P.*  
99 *destructans* invasion and establishment to capture pathogen accumulation in the environmental  
100 reservoir across 21 sites in the Midwestern, United States. Using these data, we explored  
101 potential differences in pathogen shedding among species. We also assessed the relationship  
102 between bat infections and the amount of pathogen shed into the environment by each species  
103 present in the community. Because we hypothesized that bat species abundance would play a key

104 role in site-level contamination and pathogen establishment of the environmental reservoir, we  
105 also explored how differential pathogen shedding among species and their abundance influences  
106 the pathogen pressure within the community.

107

## 108 **Methods**

### 109 *Sample collection and quantification*

110 We quantified *P. destructans* fungal loads on bats and from hibernacula substrate  
111 throughout bat hibernation sites in the Midwestern, United States. Samples were collected from  
112 21 sites in Wisconsin, Illinois, and Michigan over seven years from pathogen invasion to  
113 establishment. Hibernacula were visited twice yearly, once during early hibernation (November  
114 to December) and once during late hibernation (March to April) to capture differences in  
115 infection and environmental contamination at the beginning and end of hibernation. During each  
116 visit, we counted the total number of bats within each site by species (*Eptesicus fuscus*, *Myotis*  
117 *lucifugus*, *Myotis septentrionalis* and *Perimyotis subflavus*). We collected epidermal swab  
118 samples from bats within sites to quantify bat infections (fungal loads) and determine infection  
119 prevalence. Samples were collected using previously established protocols that consisted of  
120 rubbing a polyester swab dipped in sterile water over the muzzle and forearm of the bat five  
121 times (Langwig et al. 2015a, Hoyt et al. 2016).

122 We also collected environmental substrate swabs from hibernacula walls and ceilings  
123 directly under hibernating bats to measure the amount of *P. destructans* shed into the  
124 environment. To capture site-level environmental contamination, *P. destructans* was collected  
125 from the environment in locations more than two meters away from any roosting bats, but in  
126 areas that bats might roost. These environmental substrate samples were taken by swabbing an

127 area of substrate equal to the length of a bat's forearm (36-40 mm) five times back and forth, as  
128 described previously (Langwig et al. 2015b). We preserved *P. destructans* DNA samples by  
129 storing all swabs in salt preservation buffer (RNAlater; Thermo Fisher Scientific) directly after  
130 collection. DNA was extracted from all samples with a modified Qiagen DNeasy Blood &  
131 Tissue Kit (Langwig et al. 2015b). The presence and quantity of *P. destructans* was determined  
132 by quantitative Polymerase Chain Reaction (qPCR) (Muller et al. 2013).

133 To verify that fungal loads measured using qPCR accurately reflected viable fungal  
134 spores in the environment, that would be capable of infecting a host, we collected additional  
135 substrate swab samples from a subset of locations that were paired with swabs used for qPCR.  
136 These samples were cultured by streaking the substrate swab across a plate containing Sabouraud  
137 Dextrose Agar treated with chloramphenicol and gentamicin. The plates were stored at 4 °C and  
138 colony forming units (CFU's) of *P. destructans* were quantified within six weeks of initial  
139 inoculation. We paired substrate samples analyzed using qPCR to determine  $\log_{10}$  *P. destructans*  
140 loads for comparison with colony forming units obtained from culture samples to validate  
141 viability. There was a significant relationship between quantity of DNA measured through qPCR  
142 and the number of *P. destructans* CFU's (Figure S1). This suggests that qPCR was a valid  
143 method to estimate the extent of *P. destructans* in the environment and supports that qPCR  
144 results are reflective of the number of infectious propagules in the environment and not relic  
145 DNA (Figure S1).

146 All research was approved through Institutional Animal Care and Use Committee  
147 protocols: Virginia Polytechnic Institute: 17-180; University of California, Santa Cruz:  
148 Kilpm1705; Wisconsin Endangered/Threatened Species Permit 882 & 886; Michigan  
149 Department of Natural Resources permit SC-1651; Illinois Endangered/ Threatened Species

150 Permit 5015, 2582 and Scientific Collections permit NH20.5888; US Fish and Wildlife Service  
151 Threatened & Endangered Species Permit TE64081B-1.

152 *Data analysis*

153 We separated invasion stage into two distinct categories: “invasion” which included the  
154 first year the pathogen arrived, as described previously (Langwig et al. 2015b, Hoyt et al. 2020),  
155 and “establishment” which included the second and third years of *P. destructans* presence in a  
156 site when species declines begin to occur, which corresponds to the epidemic phase as has been  
157 previously noted (Langwig et al. 2015b, Hoyt et al. 2020). We used these stages to capture  
158 pathogen shed into the environment before and after pathogen accumulation in the environment  
159 occurred (invasion and establishment, respectively) and to examine the dynamic changes  
160 between stages of pathogen invasion and establishment.

161 We first examined the presence and quantity of *P. destructans* on each species and the  
162 amount each species shed into the environment. We used mixed effect models with  $\log_{10}$   
163 environmental fungal load collected under each bat as our response variable, bat species  
164 interacting with pathogen invasion stage as our predictor and site as a random effect. We  
165 similarly compared infection intensity among species using the same model as described above,  
166 but with  $\log_{10}$  fungal loads on bats as the response variable. We examined differences in  
167 infection prevalence by species using a generalized linear mixed effects model with a binomial  
168 distribution and a logit link with species as our predictor and bat infection prevalence (0|1) as our  
169 response and site as a random effect.

170 To examine how differences in infection on each bat contributed to contamination of the  
171 environment under each individual, we used a linear mixed effects model to explore the  
172 relationship between infection on each individual bat and pathogen shed into the environment

173 under each individual. In this analysis, we used paired  $\log_{10}$  environmental *P. destructans* loads  
174 under a bat as our response variable with  $\log_{10}$  bat fungal loads interacting with species as our  
175 predictor and site as a random effect. We combined the invasion and established stages since the  
176 amount of pathogen shed into the environment was hypothesized to be a product of how infected  
177 the host was, and therefore, comparable across years.

178 We investigated the role of species abundance in environmental contamination of *P.*  
179 *destructans*. We tested for differences among species abundance within each site by using a  
180 linear mixed effects model with species as our predictor and  $\log_{10}$  average abundance during  
181 early hibernation (before over-winter declines occur) as our response and included site as a  
182 random effect for both invasion stages. To explore how species abundance influenced the degree  
183 of pathogen contamination within sites, we used a linear mixed effect model with  $\log_{10}$   
184 environmental fungal loads collected > 2m from any bat during late hibernation as our response  
185 variable and  $\log_{10}$  average abundance interacting with species identity as our predictors with site  
186 as a random effect.

187 Finally, we calculated differences in propagule pressure among species by multiplying  
188 infection prevalence by the species abundance within each site to get the number of infected  
189 individuals. We then multiplied the number of infected individuals by the average amount of  
190 fungal spores (conidia) shed into the environment by each species in each site. We used a  
191 generalized linear mixed effect model with a negative binomial distribution to account for  
192 dispersed counts with an interaction between invasion stage and species as our predictor and  
193 propagule pressure as our response. We performed this analysis for both invasion and  
194 establishment during late hibernation to investigate how pathogen pressure may differ across  
195 stages of pathogen invasion when bats are heavily shedding into the environment. To assess if

196 propagule pressure was a suitable metric for pathogen invasion of the environmental reservoir,  
197 we examined the relationship between site-level environmental contamination, as described  
198 above, and sum propagule pressure for each site using a linear mixed effects model with site  
199 included as a random effect. All analyses were conducted in R v.4.2.1 (R Core Team 2022).  
200 Mixed-effects models were run using the package “lme4” (Bates et al. 2015) except for analyses  
201 using a negative binomial distribution which were ran using “glmmTMB” (Brooks et al. 2017)  
202

203 **Results**

204 We found that pathogen shedding (the amount of pathogen under bats) varied among the  
205 four species (Figure 1). During initial pathogen invasion into bat communities, we found that on  
206 average individual *M. septentrionalis* (Figure 1A; Table S1; intercept =  $-3.79 \pm 0.23$ ) contributed  
207 more pathogen into the environment than *E. fuscus* (coeff =  $-0.77 \pm 0.37$ ,  $P = 0.04$ ) and *M.*  
208 *lucifugus* (coeff =  $-0.58 \pm 0.27$ ,  $P = 0.03$ ), but did not differ statistically from individual *P.*  
209 *subflavus* (coeff =  $-0.21 \pm 0.38$ ,  $P = 0.58$ ). In the established stage (Figure 1B), we found support  
210 for higher shedding in *M. lucifugus* (intercept =  $-3.38 \pm 0.11$ ) than *E. fuscus* (coeff =  $-0.80 \pm$   
211  $0.14$ ,  $P < 0.0001$ ) and *P. subflavus* (coeff =  $-0.62 \pm 0.13$ ,  $P < 0.0001$ ), but similar shedding to *M.*  
212 *septentrionalis* (coeff =  $-0.38 \pm 0.24$ ,  $P = 0.11$ ).

213 Our results showed consistent support that host infection intensity predicted the amount  
214 of pathogen shed into the environment for all species (Figure 2C; Table S4; host infection and  
215 shedding relationship: *M. lucifugus* slope =  $0.38 \pm 0.05$ ,  $P < 0.001$ ; *E. fuscus* slope =  $0.33 \pm 0.07$ ,  
216  $P < 0.00001$ ; *M. septentrionalis* slope =  $0.41 \pm 0.10$ ,  $P = 0.00003$ ; *P. subflavus* slope =  $0.33 \pm$   
217  $0.08$ ,  $P = 0.00006$ ). Importantly, we found no support for differences among species in the slope  
218 between environmental pathogen shedding and host infection level (Figure 2C; Table S4; all  $P >$

219 0.05), suggesting that differences in shedding were primarily driven by the extent of infection on  
220 individual bats. *Eptesicus fuscus* (intercept =  $-3.37 \pm 0.16$ ) had significantly lower infection  
221 levels than all other species within the community (Figure 2B; Table S3; *M. lucifugus* coeff =  
222  $1.38 \pm 0.15$ ,  $P < 0.0001$ ; *M. septentrionalis* coeff =  $1.08 \pm 0.21$ ,  $P < 0.0001$ ; *P. subflavus* coeff =  
223  $1.30 \pm 0.17$ ,  $P < 0.0001$ ) In addition, we found that *M. lucifugus* (intercept =  $2.19 \pm 0.27$ ) had the  
224 highest infection prevalence, with 87% of hosts infected on average across the invasion and  
225 established stages (Figure 2A; Table S2; *E. fuscus* coeff =  $-0.79 \pm 0.31$ ,  $P < 0.01$ ; *M.*  
226 *septentrionalis* coeff =  $-0.83 \pm 0.35$ ,  $P < 0.05$ ; *P. subflavus* coeff =  $-1.10 \pm 0.24$ ,  $P < 0.0001$ ).

227 In addition to differences in infection intensity, species also varied in abundance, with *M.*  
228 *lucifugus* (intercept =  $1.63 \pm 0.19$ ) being the most abundant species across sites, with an average  
229 population size of  $39.81 \pm 7.76$  before declines from WNS (invasion) (Figure 3; Table S5; *E.*  
230 *fuscus* coeff =  $-0.65 \pm 0.24$ ,  $P < 0.01$ ; *M. septentrionalis* coeff =  $-0.60 \pm 0.21$ ,  $P < 0.01$ ; *P.*  
231 *subflavus* coeff =  $-0.41 \pm 0.23$ ,  $P < 0.08$ ). During the established stage, while population declines  
232 were occurring, *M. lucifugus* (intercept =  $1.28 \pm 0.13$ ) remained the most abundant species  
233 within the community with an average population size of  $18.20 \pm 7.41$  (Figure 3; Table S6; *E.*  
234 *fuscus* coeff =  $-0.54 \pm 0.16$ ,  $P < 0.001$ ; *M. septentrionalis* coeff =  $-0.76 \pm 0.14$ ,  $P < 0.0001$ ; *P.*  
235 *subflavus* coeff =  $-0.38 \pm 0.15$ ,  $P < 0.01$ ). *M. septentrionalis* had the lowest abundance in the  
236 community with an average colony size of  $11.22 \pm 5.50$  individuals before disease impacts and  
237 declined to an average of  $3.52 \pm 4.12$  individuals in a site during the established stage (Figure 3;  
238 Table S5-7). Furthermore, host abundance was important in influencing the degree of site-level  
239 environmental pathogen contamination (Figure S2; Table S7; *M. lucifugus* slope =  $0.40 \pm 0.14$ ,  $P$   
240 = 0.03).

241 Finally, when we combined infection prevalence, species abundance, and pathogen  
242 shedding into the metric of propagule pressure, we found that during the first year of invasion,  
243 *M. septentrionalis* (Figure 4A; Table S8; intercept =  $7.85 \pm 0.66$ ) had higher propagule pressure  
244 than *P. subflavus* (coeff =  $-2.81 \pm 1.01$ ,  $P < 0.01$ ) and *E. fuscus* ( $-4.28 \pm 0.85$ ,  $P < 0.0001$ ), but  
245 not *M. lucifugus* (coeff =  $0.43 \pm 0.73$ ,  $P = 0.55$ ). In years following invasion, once *P. destructans*  
246 is established, *M. lucifugus* (Figure 4B; intercept =  $11.08 \pm 0.56$ ) had consistently higher  
247 propagule pressure and contributed more pathogen to the environmental reservoir than all other  
248 species (Figure 4B; *M. septentrionalis* coeff =  $-4.14 \pm 0.96$ ,  $P < 0.0001$ ; *E. fuscus* coeff =  $-4.18 \pm$   
249  $0.68$ ,  $P < 0.0001$ ; *P. subflavus* coeff =  $-2.53 \pm 0.68$ ,  $P = 0.002$ ). *Myotis septentrionalis* (Figure  
250 4B; intercept =  $6.94 \pm 0.95$ ) no longer contributed more than *P. subflavus* (coeff =  $1.62 \pm 1.03$ ,  $P$   
251 =  $0.11$ ) and *E. fuscus* (coeff =  $-0.04 \pm 1.02$ ,  $P = 0.97$ ) due to their rarity following disease-  
252 induced declines (Figure 4). Mean environmental contamination in areas  $> 2\text{m}$  from bats  
253 increased with total propagule pressure at a site (summed propagule pressure among species)  
254 (Figure 4C; relationship between environmental contamination and propagule pressure intercept  
255 =  $-5.48 \pm 0.14$ , slope =  $0.12$ ,  $P = 0.002$ ).

256

257 ***Discussion***

258 Host heterogeneity in pathogen shedding and subsequent environmental transmission can  
259 have dramatic impacts on community-level disease outcomes. Our findings demonstrate how  
260 host heterogeneity in infection intensity can lead to increased pathogen shedding, which is  
261 consistent with research in other systems (Lloyd-Smith et al. 2005, Matthews et al. 2006, Chase-  
262 Topping et al. 2008, Direnzo et al. 2014, Munywoki et al. 2015, Maguire et al. 2016,  
263 VanderWaal and Ezenwa 2016). In addition, our study demonstrates that host heterogeneities in

264 abundance and infection interact to influence the extent of the environmental reservoir and the  
265 contribution of species, which varied over time. We identified a shift in the species responsible  
266 for the greatest environmental reservoir contamination between disease stages, suggesting that  
267 reservoir contamination is a dynamic process that varies over time.

268 Our findings suggest that the observed heterogeneities in pathogen shedding are primarily  
269 due to variation in infection intensities among species within the community. The relationship  
270 between individual host shedding into the environment and host infection intensity did not differ  
271 among species, suggesting that individuals of different species with the same infection intensity  
272 are equally efficient at depositing pathogen into the environment. Instead, the severity of  
273 infection, which varied among species, determined how much pathogen is shed per individual.  
274 Some species such as *E. fuscus* had low level infections, while the other species such as *M.*  
275 *septentrionalis* and *M. lucifugus* were much more infected and contributed more pathogen to the  
276 environmental reservoir (Figure 2B).

277 Disease-caused declines in several species (Figure 3) resulted in large changes in species  
278 abundance and community composition. We found evidence that species abundance predicted  
279 site-level contamination (Figure S2), and this supported the need to account for both species'  
280 infection and abundance when determining the contribution to the environmental reservoir. To  
281 combine these factors, we used propagule pressure or "introduction effort" which is a  
282 fundamental ecological metric that determines whether a biological invasion will be successful in  
283 reaching establishment (Lockwood et al. 2005), and is especially applicable to emerging  
284 infectious diseases. Our results indicated that during the initial invasion of *P. destructans*, both  
285 *M. lucifugus* and *M. septentrionalis* had higher propagule pressure than the other two species  
286 (Figure 4A), which was not apparent through examination of only pathogen shedding. The high

287 infection levels of *M. septentrionalis* resulted in a large contribution to the initial establishment  
288 of the environmental reservoir despite their low relative abundance (Figure 2B; Figure 3).  
289 However, in subsequent years, as this species declined precipitously (Figure 3), their  
290 contribution was greatly reduced and equivalent to less infected species (e.g. *E. fuscus* and *P.*  
291 *subflavus*, Figure 4B).

292 Our results suggest that host abundance, shedding, and infection prevalence are  
293 collectively required to describe pathogen contamination in the environment. We found that  
294 environmental contamination in the sampled locations that were not associated with bats  
295 increased as propagule pressure increased (Figure 4C), suggesting that propagule pressure is an  
296 accurate metric for measuring species contributions to the environmental reservoir. For example,  
297 while *E. fuscus*, *M. septentrionalis*, and *P. subflavus* eventually contributed similar propagule  
298 pressures during disease establishment, this was likely driven by different factors that need to be  
299 considered when evaluating their influence on the reservoir. *Eptesicus fuscus* had low infection  
300 intensity but had moderate prevalence (Figure 2A-B) and moderate abundance (Figure 3) which  
301 elevated its contribution. *Perimyotis subflavus* had high infection levels, but reduced prevalence  
302 (Figure 2A-B) compared to the other highly infected species and was only present in moderate  
303 abundances (Figure 3). Finally, *M. septentrionalis* was highly infected (Figure 2B), but at low  
304 abundance across communities (Figure 3), which reduced its overall importance in years  
305 following initial pathogen invasion. *Myotis lucifugus* maintained high propagule pressure  
306 through the invasion and establishment of *P. destructans* (Figure 4A-B), suggesting that the  
307 presence of *M. lucifugus* within a community will result in rapid establishment of *P. destructans*  
308 in the environment and maintenance of environmental contamination within a site over time. Our  
309 results highlight how both species infection intensity and abundance must be considered to

310 evaluate the influence of pathogen shedding on environmental reservoir establishment,  
311 subsequent environmental transmission and how this can change dynamically across disease  
312 stages.

313 Understanding environmental reservoir dynamics is crucial for many globally important  
314 disease systems. Discerning how variation across species contributes to maintenance of the  
315 environmental reservoir is important in determining the extent of epidemics, predicting long-  
316 term impacts on host communities, and developing control strategies. We demonstrate that the  
317 establishment and maintenance of the environmental reservoir is strongly influenced by both  
318 heterogeneity in pathogen infection and species abundance. Evaluating these effects together  
319 through the metric of propagule pressure allowed us to capture which species within the  
320 community contributed to pathogen invasion success and ultimately the maintenance of indirect  
321 transmission which is an important driver of infection and mortality (Hoyt et al. 2018). Broadly,  
322 our results demonstrate that multiple factors of species heterogeneity can scale to influence  
323 environmental reservoir dynamics within communities.

324

325 **Acknowledgements:**

326 The research was funded by the joint NSF-NIH-NIFA Ecology and Evolution of Infectious  
327 Disease award DEB-1911853, NSF DEB-1115895, USFWS (F17AP00591), and by the NSF  
328 GRFP. We would like to acknowledge landowners for access to sites, and M.J. Kailing for  
329 assisting culture collection and B. Heeringa and D. Kirk for field assistance.

330

331

332

333 **Author Contributions:**

334 NAL and JRH wrote the original draft of the manuscript. JRH, KEL, and AMK designed  
335 methodology; NAL, JRH, KEL, AMK, JPW, HMK, JAR, JED, WHS, and JK collected the data;  
336 NAL conducted the laboratory experiment; JTF and KLP supervised and performed sample  
337 testing; NAL analyzed the data with assistance from KEL and JRH; All authors contributed  
338 critically to draft revision.

339

340 **Conflict of Interest:** The authors declare no conflicts of interest

341 **Figure captions:**

342 **Figure 1: Differences in pathogen shedding among species during reservoir invading and**  
343 **established stages.**  $\log_{10}$  *P. destructans* environmental loads (ng DNA) among species during  
344 pathogen invasion (A) and establishment (B) in late hibernation. Each point represents the  $\log_{10}$   
345 environmental *P. destructans* loads from under an individual bat. Black points represent the  
346 estimated mean and bars indicate  $\pm$  standard error for each species.

347

348 **Figure 2: Bat infection prevalence, intensity, and the relationship between host infection**  
349 **and pathogen shedding.** For all panels, bat species are displayed by color. Black points indicate  
350 mean bat infections by species and bars represent  $\pm$  standard error. (A) Bat infection prevalence  
351 for each species during pathogen invasion in late hibernation. (B) Bat  $\log_{10}$  *P. destructans* loads  
352 (ng DNA) for each species during pathogen invasion in late hibernation. (C) The relationship  
353 between  $\log_{10}$  *P. destructans* loads (ng DNA) on an individual bat and the amount of  $\log_{10}$  *P.*  
354 *destructans* (ng DNA) in the environment directly underneath each individual during pathogen  
355 invasion and establishment in late hibernation. The gray solid line shows the 1:1 line, and points  
356 along this line would indicate that the amount of *P. destructans* on bats was equivalent to the  
357 amount shed into the environment. Solid colored lines indicate statistical support for a positive  
358 relationship. Each individual bat is represented by a point.

359

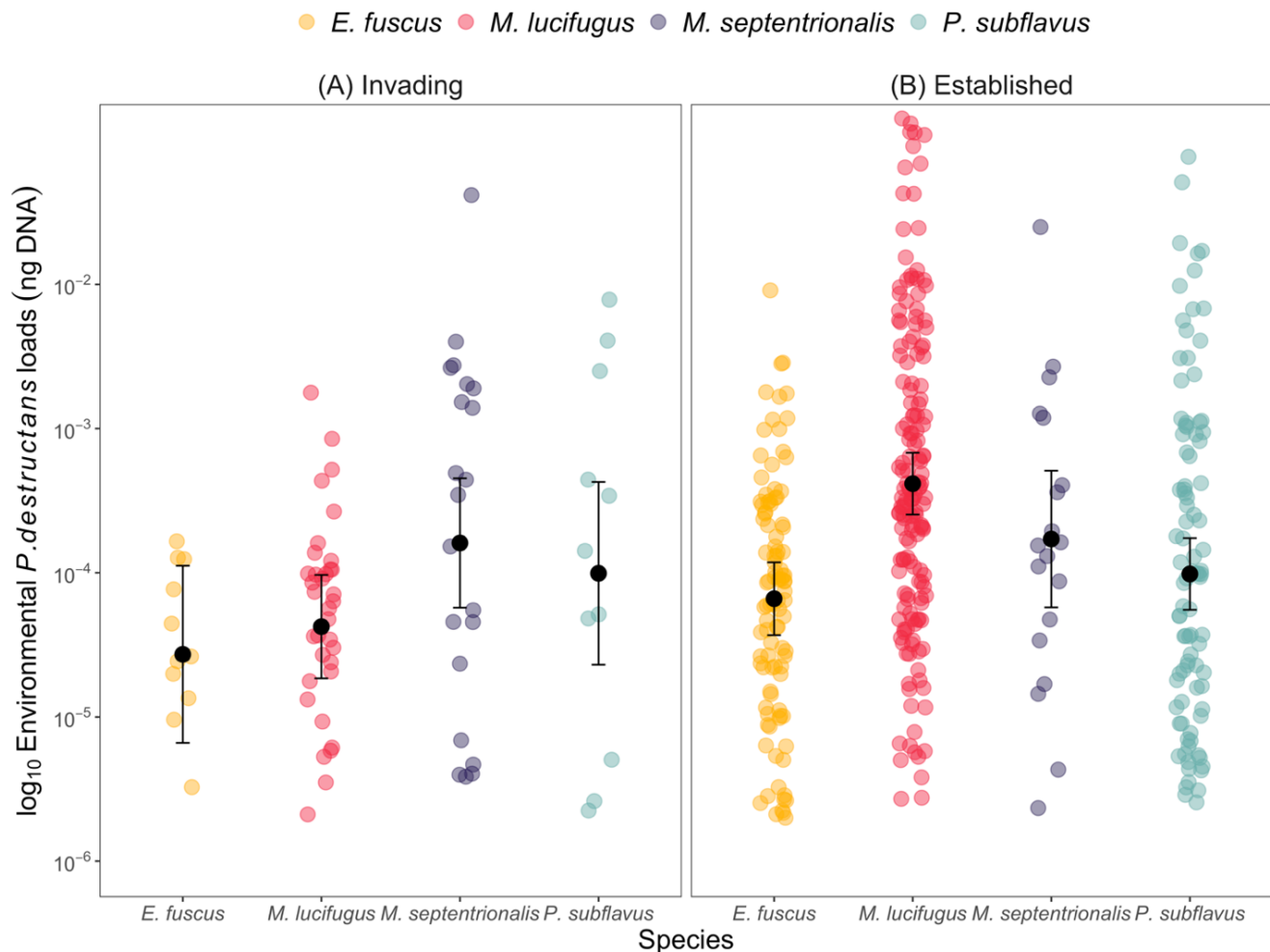
360 **Figure 3. Changes in host abundance between invading and established years.** Species  
361 within the community are differentiated by color and points represent a species population at an  
362 individual site. Species abundance in the invasion (light gray box) and established years (dark  
363 gray box) in late hibernation within each site. Circular points indicate the mean abundance for  
364 each year and bars denote  $\pm$  standard error.

365

366 **Figure 4. Differences in propagule pressure among species during invading and established**  
367 **stages and the relationship between propagule pressure and environmental contamination.**  
368 (A-B) Propagule pressure (# of pathogen particles) by species during late hibernation in (A)  
369 invading and (B) established stages. Colored points represent populations of species within a  
370 site, black points represent the mean and bars indicate  $\pm$  standard error for each species. Point  
371 size is weighted by species population abundance. (C) Relationship between  $\log_{10}$  propagule

372 pressure and  $\log_{10}$  mean site-level contamination. Site-level contamination was assessed in  
373 samples > 2m away from roosting bats within sites during late hibernation in the established  
374 stage. Points indicate the sum propagule pressure at a site for each year and shape denotes  
375 invasion stage. The total environmental contamination increased as propagule pressure increased  
376 within a site (Environmental contamination: intercept =  $-5.48 \pm 0.14$ , slope = 0.12, relationship  
377 between environmental contamination and propagule pressure  $P = 0.002$ ).

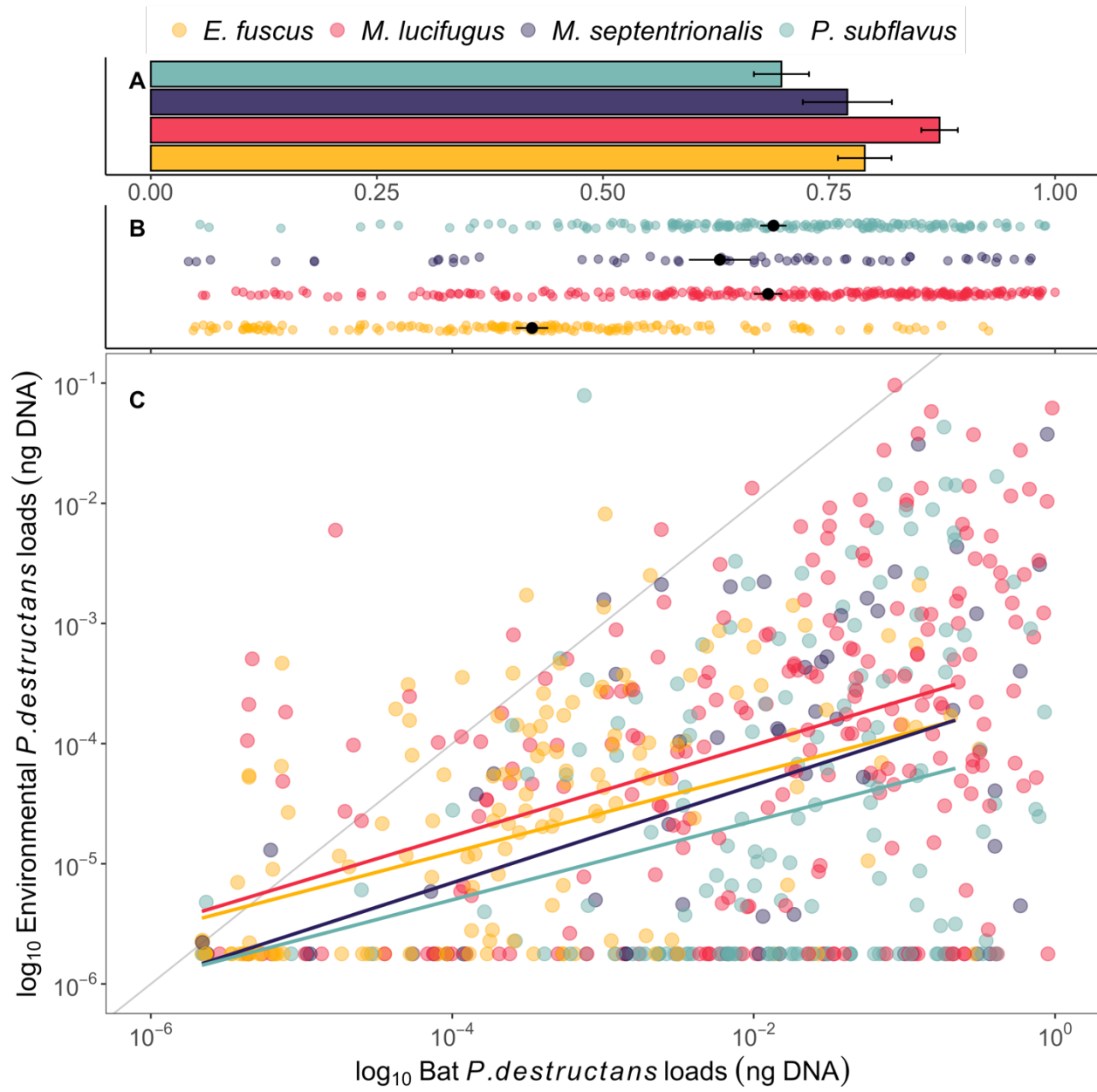
378 **Figure 1**



379

380 **Figure 2**

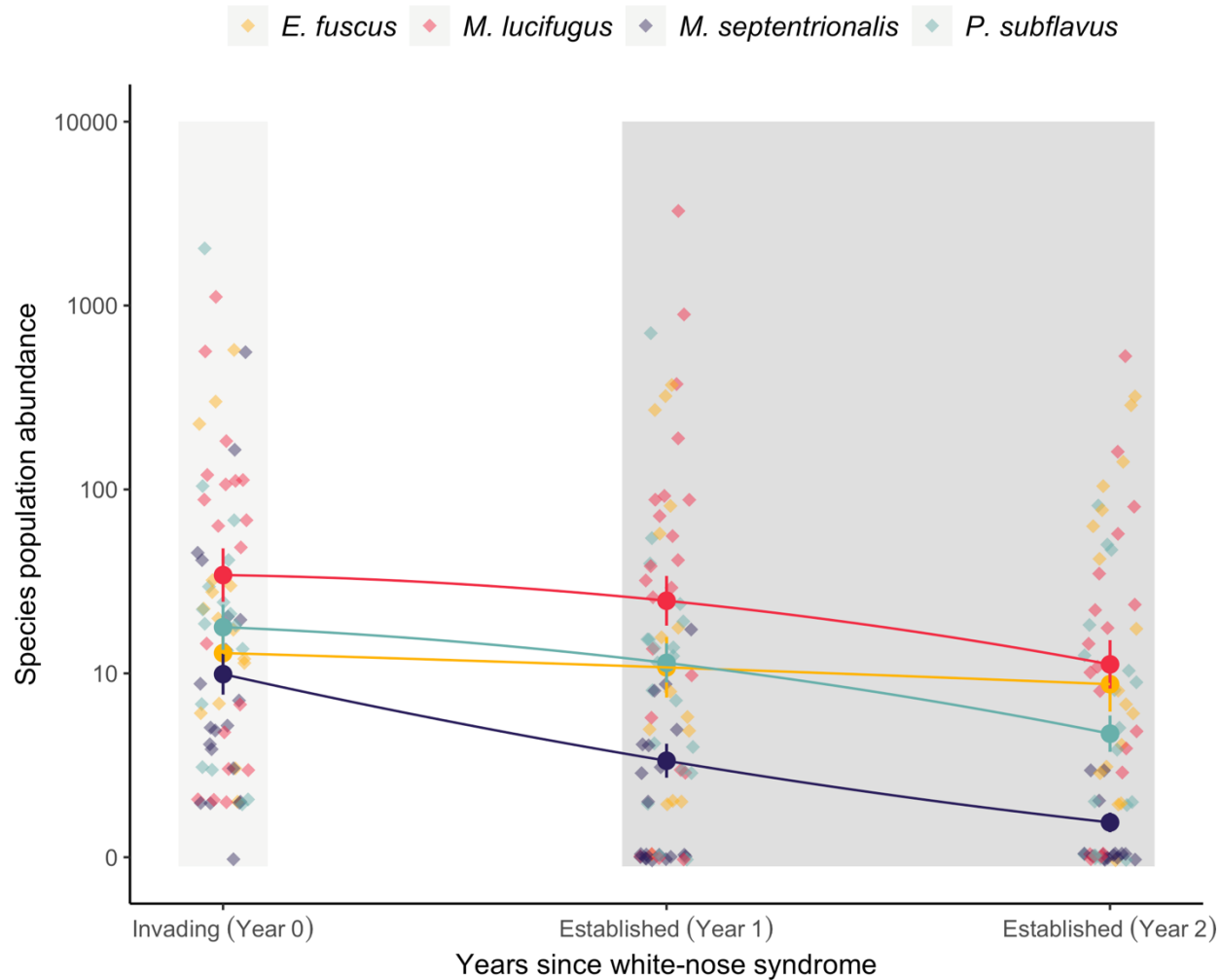
381



382

383

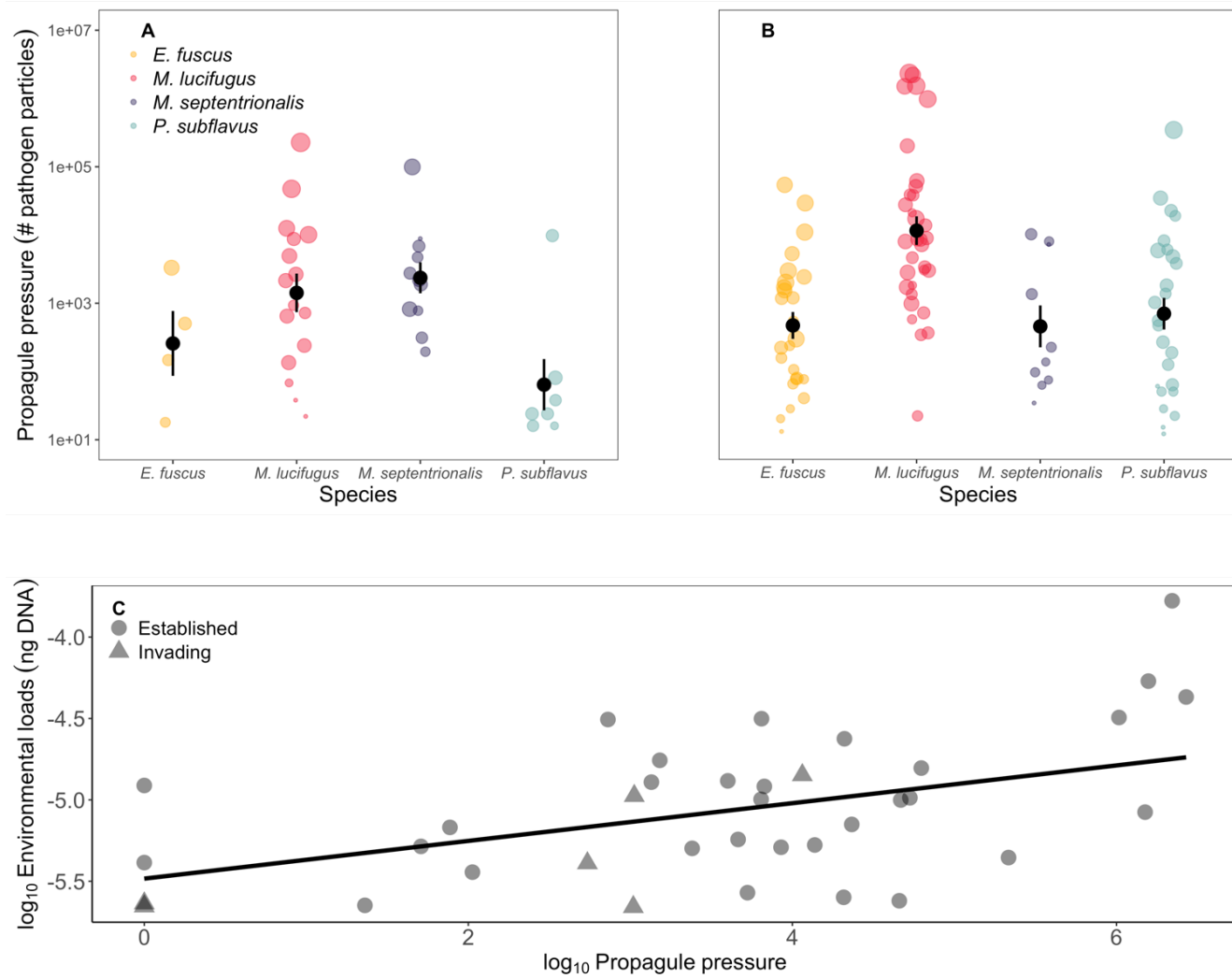
384 **Figure 3**



385

386

387 **Figure 4**



388

389

390 **References**

391 Almberg, E. S., P. C. Cross, C. J. Johnson, D. M. Heisey, and B. J. Richards. 2011. Modeling routes of  
392 chronic wasting disease transmission: environmental prion persistence promotes deer  
393 population decline and extinction. *PLoS One* **6**:e19896.

394 Bates, D., M. Mächler, B. M. Bolker, and S. C. Walker. 2015. Fitting linear mixed-effects models using  
395 lme4. *Journal of Statistical Software* **67**:1-48.

396 Brannelly, L. A., H. I. McCallum, L. F. Grogan, C. J. Briggs, M. P. Ribas, M. Hollanders, T. Sasso, M. Familiar  
397 López, D. A. Newell, and A. M. Kilpatrick. 2020. Mechanisms underlying host persistence  
398 following amphibian disease emergence determine appropriate management strategies.  
399 *Ecology Letters*.

400 Brooks, M. E., K. Kristensen, K. J. van Benthem, A. Magnusson, C. W. Berg, A. Nielson, H. J. Skaug, M.  
401 Maechler, and B. M. Bolker. 2017. glmmTMB Balances Speed and Flexibility Among Packages for  
402 Zero-inflated Generalized Linear Mixed Modeling. *The R Journal* **9**:378-400.

403 Brooks-Pollock, E., G. O. Roberts, and M. J. Keeling. 2014. A dynamic model of bovine tuberculosis  
404 spread and control in Great Britain. *Nature* **511**:228-231.

405 Campbell, L. J., D. P. Walsh, D. S. Blehert, and J. M. Lorch. 2019. Long-term survival of  
406 *Pseudogymnoascus destructans* at elevated temperatures. *Journal of Wildlife Diseases*.

407 Chase-Topping, M., D. Gally, C. Low, L. Matthews, and M. Woolhouse. 2008. Super-shedding and the link  
408 between human infection and livestock carriage of *Escherichia coli* O157. *Nat Rev Microbiol*  
409 **6**:904-912.

410 Daszak, P., A. A. Cunningham, and A. D. Hyatt. 2000. Emerging infectious diseases of wildlife - threats to  
411 biodiversity and human health. *Science* **287**:443.

412 de Castro, F., and B. Bolker. 2005. Mechanisms of disease-induced extinction. *Ecology Letters* **8**:117-126.

413 Direnzo, G. V., P. F. Langhammer, K. R. Zamudio, and K. R. Lips. 2014. Fungal infection intensity and  
414 zoospore output of *Atelopus zeteki*, a potential acute chytrid supershedder. *PLoS One* **9**:e93356.

415 Fisher, M. C., D. A. Henk, C. J. Briggs, J. S. Brownstein, L. C. Madoff, S. L. McCraw, and S. J. Gurr. 2012.  
416 Emerging fungal threats to animal, plant and ecosystem health. *Nature* **484**:186-194.

417 Frick, W. F., S. J. Puechmaille, J. R. Hoyt, B. A. Nickel, K. E. Langwig, J. T. Foster, K. E. Barlow, T.  
418 Bartonicka, D. Feller, A. J. Haarsma, C. Herzog, I. Horacek, J. van der Kooij, B. Mulkens, B. Petrov,  
419 R. Reynolds, L. Rodrigues, C. W. Stihler, G. G. Turner, and A. M. Kilpatrick. 2015. Disease alters  
420 macroecological patterns of North American bats. *Global Ecology and Biogeography* **24**:741-749.

421 Gervasi, S. S., J. Urbina, J. Hua, T. Chestnut, R. A. Relyea, and A. R. Blaustein. 2013. Experimental  
422 evidence for American bullfrog (*Lithobates catesbeianus*) susceptibility to chytrid fungus  
423 (*Batrachochytrium dendrobatidis*). *Ecohealth* **10**:166-171.

424 Godfrey, S. S. 2013. Networks and the ecology of parasite transmission: A framework for wildlife  
425 parasitology. *Int J Parasitol Parasites Wildl* **2**:235-245.

426 Henaux, V., and M. D. Samuel. 2011. Avian influenza shedding patterns in waterfowl: implications for  
427 surveillance, environmental transmission, and disease spread. *J Wildl Dis* **47**:566-578.

428 Hicks, A. C., S. Darling, J. Flewelling, R. von Linden, C. U. Meteyer, D. Redell, J. P. White, J. Redell, R.  
429 Smith, D. Blehert, N. Rayman, J. R. Hoyt, J. C. Okoniewski, and K. E. Langwig. 2021.  
430 Environmental transmission of *Pseudogymnoascus destructans* to hibernating little brown bats.  
431 biorxiv.

432 Hoyt, J. R., A. M. Kilpatrick, and K. E. Langwig. 2021. Ecology and impacts of white-nose syndrome on  
433 bats. *Nature Reviews Microbiology*:1-15.

434 Hoyt, J. R., K. E. Langwig, J. Okoniewski, W. F. Frick, W. B. Stone, and A. M. Kilpatrick. 2015. Long-term  
435 persistence of *Pseudogymnoascus destructans*, the causative agent of white-nose syndrome, in  
436 the absence of bats. *Ecohealth* **12**:330-333.

437 Hoyt, J. R., K. E. Langwig, K. Sun, G. Lu, K. L. Parise, T. Jiang, W. F. Frick, J. T. Foster, J. Feng, and A. M.  
438 Kilpatrick. 2016. Host persistence or extinction from emerging infectious disease: insights from  
439 white-nose syndrome in endemic and invading regions. *Proceedings of the Royal Society B: Biological Sciences* **283**.

440 Hoyt, J. R., K. E. Langwig, K. Sun, K. L. Parise, A. Li, Y. Wang, X. Huang, L. Worledge, H. Miller, J. P. White,  
441 H. M. Kaarakka, J. A. Redell, T. Görföl, S. A. Boldogh, D. Fukui, M. Sakuyama, S. Yachimori, A.  
442 Sato, M. Dalannast, A. Jargalsaikhan, N. Batbayar, Y. Yovel, E. Amichai, I. Natradze, W. F. Frick, J.  
443 T. Foster, J. Feng, and A. M. Kilpatrick. 2020. Environmental reservoir dynamics predict global  
444 infection patterns and population impacts for the fungal disease white-nose syndrome.  
445 *Proceedings of the National Academy of Sciences*:201914794.

446 Hoyt, J. R., K. E. Langwig, J. P. White, H. M. Kaarakka, J. A. Redell, A. Kurta, J. E. DePue, W. H. Scullon, K.  
447 L. Parise, and J. T. Foster. 2018. Cryptic connections illuminate pathogen transmission within  
448 community networks. *Nature*:1.

449 Islam, M. S., M. H. Zaman, M. S. Islam, N. Ahmed, and J. D. Clemens. 2020. Environmental reservoirs of  
450 *Vibrio cholerae*. *Vaccine* **38 Suppl 1**:A52-A62.

451 Jones, K. E., N. G. Patel, M. A. Levy, A. Storeygard, D. Balk, J. L. Gittleman, and P. Daszak. 2008. Global  
452 trends in emerging infectious diseases. *Nature* **451**:990-U994.

453 Kilonzo, C., X. Li, E. J. Vivas, M. T. Jay-Russell, K. L. Fernandez, and E. R. Atwill. 2013. Fecal shedding of  
454 zoonotic food-borne pathogens by wild rodents in a major agricultural region of the central  
455 California coast. *Appl Environ Microbiol* **79**:6337-6344.

456 Kilpatrick, A. M., P. Daszak, M. J. Jones, P. P. Marra, and L. D. Kramer. 2006. Host heterogeneity  
457 dominates West Nile virus transmission. *Proceedings of the Royal Society B-Biological Sciences*  
458 **273**:2327-2333.

459 Langwig, K. E., W. F. Frick, J. T. Bried, A. C. Hicks, T. H. Kunz, and A. M. Kilpatrick. 2012. Sociality, density-  
460 dependence and microclimates determine the persistence of populations suffering from a novel  
461 fungal disease, white-nose syndrome. *Ecol Lett* **15**.

462 Langwig, K. E., W. F. Frick, J. R. Hoyt, K. L. Parise, K. P. Drees, T. H. Kunz, J. T. Foster, and A. M. Kilpatrick.  
463 2016. Drivers of variation in species impacts for a multi-host fungal disease of bats. *Philosophical  
464 Transactions of the Royal Society B: Biological Sciences* **10.1098/rstb.2015.0456**.

465 Langwig, K. E., W. F. Frick, R. Reynolds, K. L. Parise, K. P. Drees, J. R. Hoyt, T. L. Cheng, T. H. Kunz, J. T.  
466 Foster, and A. M. Kilpatrick. 2015a. Host and pathogen ecology drive the seasonal dynamics of a  
467 fungal disease, white-nose syndrome. *Proceedings of the Royal Society B: Biological Sciences*  
468 **282**:20142335.

469 Langwig, K. E., J. R. Hoyt, K. L. Parise, J. Kath, D. Kirk, W. F. Frick, J. T. Foster, and A. M. Kilpatrick. 2015b.  
470 Invasion Dynamics of White-Nose Syndrome Fungus, Midwestern United States, 2012-2014.  
471 *Emerging Infectious Disease* **21**:1023-1026.

472 Langwig, K. E., J. P. White, K. L. Parise, H. M. Kaarakka, J. A. Redell, J. E. DePue, W. H. Scullon, J. T. Foster,  
473 A. M. Kilpatrick, and J. R. Hoyt. 2021. Mobility and infectiousness in the spatial spread of an  
474 emerging fungal pathogen. *J Anim Ecol* **90**:1134-1141.

475 Lawley, T. D., D. M. Bouley, Y. E. Hoy, C. Gerke, D. A. Relman, and D. M. Monack. 2008. Host  
476 transmission of *Salmonella enterica* serovar *Typhimurium* is controlled by virulence factors and  
477 indigenous intestinal microbiota. *Infect Immun* **76**:403-416.

478 Lloyd-Smith, J. O., S. J. Schreiber, P. E. Kopp, and W. M. Getz. 2005. Superspreading and the effect of  
479 individual variation on disease emergence. *Nature* **438**:355-359.

480 Lockwood, J. L., P. Cassey, and T. Blackburn. 2005. The role of propagule pressure in explaining species  
481 invasions. *Trends Ecol Evol* **20**:223-228.

483 Lorch, J. M., C. U. Meteyer, M. J. Behr, J. G. Boyles, P. M. Cryan, A. C. Hicks, A. E. Ballmann, J. T. H.  
484 Coleman, D. N. Redell, D. M. Reeder, and D. S. Blehert. 2011. Experimental infection of bats with  
485 *Geomycetes destructans* causes white-nose syndrome. *Nature* **480**:376-378.  
486 Lorch, J. M., L. K. Muller, R. E. Russell, M. O'Connor, D. L. Lindner, and D. S. Blehert. 2013. Distribution  
487 and environmental persistence of the causative agent of white-nose syndrome, *Geomycetes*  
488 *destructans*, in bat hibernacula of the eastern United States. *Applied and Environmental*  
489 *Microbiology* **79**:1293-1301.  
490 Maguire, C., G. V. DiRenzo, T. S. Tunstall, C. R. Muletz-Wolz, K. R. Zamudio, and K. R. Lips. 2016. Dead or  
491 alive? Viability of chytrid zoospores shed from live amphibian hosts. *Diseases of Aquatic*  
492 *Organisms* **199**:179-187.  
493 Matthews, L., J. C. Low, D. L. Gally, M. C. Pearce, D. J. Mellor, J. A. Heesterbeek, M. Chase-Topping, S. W.  
494 Naylor, D. J. Shaw, S. W. Reid, G. J. Gunn, and M. E. Woolhouse. 2006. Heterogeneous shedding  
495 of *Escherichia coli* O157 in cattle and its implications for control. *Proc Natl Acad Sci U S A*  
496 **103**:547-552.  
497 McGuire, L. P., H. W. Mayberry, and C. K. Willis. 2017. White-nose syndrome increases torpid metabolic  
498 rate and evaporative water loss in hibernating bats. *American Journal of Physiology-Regulatory,*  
499 *Integrative and Comparative Physiology* **313**:R680-R686.  
500 Mitchell, K. M., T. S. Churcher, T. W. Garner, and M. C. Fisher. 2008. Persistence of the emerging  
501 pathogen *Batrachochytrium dendrobatidis* outside the amphibian host greatly increases the  
502 probability of host extinction. *Proc Biol Sci* **275**:329-334.  
503 Muller, L. K., J. M. Lorch, D. L. Lindner, M. O'Connor, A. Gargas, and D. S. Blehert. 2013. Bat white-nose  
504 syndrome: a real-time TaqMan polymerase chain reaction test targeting the intergenic spacer  
505 region of *Geomycetes destructans*. *Mycologia* **105**:253-259.  
506 Munywoki, P. K., D. C. Koech, C. N. Agoti, N. Kibirige, J. Kipkoech, P. A. Cane, G. F. Medley, and D. J.  
507 Nokes. 2015. Influence of age, severity of infection, and co-infection on the duration of  
508 respiratory syncytial virus (RSV) shedding. *Epidemiol Infect* **143**:804-812.  
509 Paull, S. H., S. Song, K. M. McClure, L. C. Sackett, A. M. Kilpatrick, and P. T. J. Johnson. 2012. From  
510 superspreaders to disease hotspots: linking transmission across hosts and space. *Frontiers in*  
511 *Ecology and the Environment* **10**:75-82.  
512 Peterson, A. C., and V. J. McKenzie. 2014. Investigating differences across host species and scales to  
513 explain the distribution of the amphibian pathogen *Batrachochytrium dendrobatidis*. *PLoS One*  
514 **9**:e107441.  
515 Plummer, I. H., C. J. Johnson, A. R. Chesney, J. A. Pedersen, and M. D. Samuel. 2018. Mineral licks as  
516 environmental reservoirs of chronic wasting disease prions. *PLoS One* **13**:e0196745.  
517 Rushmore, J., D. Caillaud, L. Matamba, R. M. Stumpf, S. P. Borgatti, and S. Altizer. 2013. Social network  
518 analysis of wild chimpanzees provides insights for predicting infectious disease risk. *J Anim Ecol*  
519 **82**:976-986.  
520 Scheele, B. C., D. A. Hunter, L. A. Brannelly, L. F. Skerratt, and D. A. Driscoll. 2017. Reservoir-host  
521 amplification of disease impact in an endangered amphibian. *Conserv Biol* **31**:592-600.  
522 Searle, C. L., S. S. Gervasi, J. Hua, J. I. Hammond, R. A. Relyea, D. H. Olson, and A. R. Blaustein. 2011.  
523 Differential Host Susceptibility to *Batrachochytrium dendrobatidis*, an Emerging Amphibian  
524 Pathogen. *Conservation Biology* **25**:965-974.  
525 Sheth, P. M., A. Danesh, A. Sheung, A. Rebbapragada, K. Shahabi, C. Kovacs, R. Halpenny, D. Tilley, T.  
526 Mazzulli, K. MacDonald, D. Kelvin, and R. Kaul. 2006. Disproportionately high semen shedding of  
527 HIV is associated with compartmentalized cytomegalovirus reactivation. *J Infect Dis* **193**:45-48.  
528 Slater, N., R. M. Mitchell, R. H. Whitlock, T. Fyock, A. K. Pradhan, E. Knupfer, Y. H. Schukken, and Y.  
529 Louzoun. 2016. Impact of the shedding level on transmission of persistent infections in  
530 *Mycobacterium avium* subspecies *paratuberculosis* (MAP). *Vet Res* **47**:38.

531 Taylor, L. H., S. M. Latham, and M. E. Woolhouse. 2001. Risk factors for human disease emergence.  
532 *Philos Trans R Soc Lond B Biol Sci* **356**:983-989.

533 Turner, W. C., K. L. Kausrud, W. Beyer, W. R. Easterday, Z. R. Barandongo, E. Blaschke, C. C. Cloete, J.  
534 Lazak, M. N. Van Ert, and H. H. Ganz. 2016. Lethal exposure: An integrated approach to  
535 pathogen transmission via environmental reservoirs. *Scientific reports* **6**:27311.

536 VanderWaal, K. L., and V. O. Ezenwa. 2016. Heterogeneity in pathogen transmission: mechanisms and  
537 methodology. *Funct. Ecol.* **30**:1606-1622.

538 Verant, M. L., M. U. Carol, J. R. Speakman, P. M. Cryan, J. M. Lorch, and D. S. Blehert. 2014. White-nose  
539 syndrome initiates a cascade of physiologic disturbances in the hibernating bat host. *BMC  
540 physiology* **14**:10.

541 Warnecke, L., J. M. Turner, T. K. Bollinger, J. M. Lorch, V. Misra, P. M. Cryan, G. Wibbelt, D. S. Blehert,  
542 and C. K. R. Willis. 2012. Inoculation of bats with European *Geomyces destructans* supports the  
543 novel pathogen hypothesis for the origin of white-nose syndrome. *Proceedings of the National  
544 Academy of Sciences of the United States of America* **109**:6999-7003.

545 Warnecke, L., J. M. Turner, T. K. Bollinger, V. Misra, P. M. Cryan, D. S. Blehert, G. Wibbelt, and C. K. R.  
546 Willis. 2013. Pathophysiology of white-nose syndrome in bats: a mechanistic model linking wing  
547 damage to mortality. *Biology Letters* **9**.

548